Experimental Gerontology 168 (2022) 111944

Contents lists available at ScienceDirect

Experimental Gerontology

journal homepage: www.elsevier.com/locate/expgero

Phosphonate analog of 2-oxoglutarate regulates glutamate-glutamine homeostasis and counteracts amyloid beta induced learning and memory deficits in rats

Fatemeh Sayehmiri [a], Fariba Khodagholi [b,*], Hamid Gholami Pourbadie [c], Nima Naderi [d], Faezeh Aliakbarzadeh [e], Reza Hashemi [a], Soudabeh Naderi [a], Fereshteh Motamedi [f,*]

[a] School of Medicine, Neuroscience Research Center, Shahid Beheshti University of Medical Sciences, Tehran, Iran
[b] Neurobilogy Research Center, Shahid Beheshti University of Medical Sciences, Tehran, Iran
[c] Department of Physiology and Pharmacology, Pasteur Institute of Iran, Tehran, Iran
[d] Department of Pharmacology and Toxicology, School of Pharmacy, Shahid Beheshti University of Medical Sciences, Tehran, Iran
[e] Department of Environmental Health Engineering, School of Public Health and Safety, Shahid Beheshti University of Medical Sciences, Tehran, Iran
[f] Neuroscience Research Center, Shahid Beheshti University of Medical Sciences, Tehran, Iran

ARTICLE INFO

Section Editor: Christiaan Leeuwenburgh

Keywords:
Alzheimer's disease
Amyloid beta
Glutamate-glutamine homeostasis
α-Ketoglutarate dehydrogenase enzyme complex
Spatial learning and memory

ABSTRACT

Background: Metabolic alteration is a mainstream concept underlying the cognitive decline in neurodegenerative disorders including Alzheimer's disease (AD). Mitochondrial enzyme α-ketoglutarate dehydrogenase complex (α-KGDHC) seems to play a dual-edged sword role in cytotoxic insult. Here, using succinyl phosphonate (SP), a specific α-KGDHC inhibitor, we aimed to examine its potential action on AD progression.

Methods: Male Wistar rats were assigned to two separate experiments. First, they were bilaterally microinjected into the dorsal CA_1 area by amyloid-beta $(A\beta)_{25-35}$ for four consecutive days. Seven days after the last injection, they were trained to acquire Morris Water Maze (MWM) task for three successive days when they were treated with SP after each training session. In the second experiment, SP was administered 30 min after the first Aβ microinjection and behavioral tests were performed one week after the last Aβ administration. The activity of glutamate dehydrogenase (GDH), and glutamine synthetase (GS), as key enzymes involved in glutamate-glutamine homeostasis and histological assays were evaluated in the hippocampi.

Results: Our behavioral results indicated that post-training SP treatment enhanced task acquisition but did not change memory performance in Aβ-treated rats. However, administration of SP at the time of Aβ injection precludes the deteriorative effect of Aβ and neuronal injury on both spatial learning and memory performances indicating its preventive action against Aβ pathology at its early stages. Measurement of enzymes activity shows that α-KGDHC activity was reduced in the Aβ treated group, and SP administration restored its activity; also, GDH and GS activities were increased and decreased respectively due to Aβ, and SP reversed the action of Aβ on these enzymes.

Conclusions: This study proposes that SP possibly a promising therapeutic approach to improve memory impairment in AD, especially in the early phases of this disease.

1. Introduction

Changes in brain mitochondrial enzyme α-ketoglutarate dehydrogenase complex (α-KGDHC) activity, is well-known in the age-related neurodegenerative disorders including Alzheimer's disease (AD) (Shi et al., 2009; Bubber et al., 2005; Gibson et al., 1988; Mastrogiacomo et al., 1993). α-KGDHC acts as a key and often rate limiting enzyme in the Krebs cycle which links the oxidative decarboxylation of α-ketoglutarate to succinyl CoA, and the metabolism of glutamate to the Krebs cycle (Gibson et al., 1988; Gibson et al., 2013; Gibson et al., 2003; Albers

Abbreviations: SP, succinyl phosphonate; α-KGDHC, α-ketoglutarate dehydrogenase complex; Aβ, amyloid-beta; MWM, Morris's water maze; GS, glutamine synthetase; GDH, Glutamate dehydrogenase.

* Corresponding authors.
E-mail addresses: khodagholi@sbmu.ac.ir (F. Khodagholi), motamedi@ams.ac.ir (F. Motamedi).

https://doi.org/10.1016/j.exger.2022.111944
Received 17 May 2022; Received in revised form 28 July 2022; Accepted 24 August 2022
Available online 3 September 2022

et al., 2000; Park et al., 2001; Nilsen et al., 2011). Its reduced activity may alter the transfer of carbon from glutamate and glucose in the Krebs cycle (Gibson et al., 2000). Considering the function of glutamate as a neurotransmitter and the importance of glucose as the exclusive source of energy for the brain, the alterations in the function of Krebs cycle may help to find the possible relationships between the activity of α-KGDHC and brain metabolism (Gibson et al., 2000). The impairment of α-KGDHC activity causes alpha-ketoglutarate (α-KG) to enter the gamma-aminobutyric acid (GABA) shunt and increase the glutamate dehydrogenase (GDH) activity (Xiao et al., 2016). Besides, glutamate is converted to glutamine by the enzyme glutamine synthetase (GS), using ATP from the Krebs cycle (Schousboe et al., 2014). Decreased activity of α-KGDHC has been shown in the patients with dementia before death, which might be associated with decreased metabolism of brain in AD patients (Gibson et al., 1988) in both healthy and damaged brain areas (Mastrogiacomo et al., 1993; Gibson et al., 1998).

Some reports show the effect of α-KGDHC inhibition in neurodegenerative diseases such as AD depends on different durations of the inhibition (Dumont et al., 2009; Chen et al., 2016). Several studies have pointed to beneficial effects of short-term inhibition of α-KGDHC for treating neurodegenerative disorders (Chen et al., 2016; Trofimova et al., 2010; Gibson et al., 2012; Kabysheva et al., 2009). Succinyl phosphonate (SP) and its analog, carboxyethyl succinyl phosphonate (CESP), penetrate cells, and powerfully and selectively inhibit α-KGDHC. These compounds have been used in experimental model of neurodegenerative diseases to reduce α-KGDHC activity which may occur in AD (Gibson et al., 2012; Santos et al., 2006).

The α-KGDHC inhibition by SP caused behavioral changes in male rats, which was accompanied by up-regulation of the enzyme activity probably as a compensatory response (Trofimova et al., 2010). Some in vitro studies reported that mild depletion of α-KGDHC increases the level of mitochondrial protein glutathionylation by about 114 %, along with potentiation of GABA shunt and glycolysis. Conversely, glutathionylation in long-term inhibition models could not be a protective mechanism (Shi et al., 2009; Chen et al., 2016). In another study, the protective role of SP has been shown in cerebellar granule cells when exposed to glutamate toxicity. This protective effect presumably is mediated via slowing down mitochondria to enter the irreversible dysfunction. On the other hand, it has been reported that increased exposure time of neurons to SP, or an increase in SP concentration, leads to increased intracellular calcium levels. In addition, SP may act as a calcium antagonist (Kabysheva et al., 2009). Moreover, it has been reported that acute inhibition of the α-KGDHC in the N_2a cells (a mouse neural crest-derived cell line) by CESP protects cells from cell death due to oxidative stress (Chen et al., 2016).

So far, to our knowledge, there is no investigation to examine if in vivo SP administration could exert the protective effects against memory impairment in amyloid pathology. Considering the positive effects of α-KGDHC inhibition in in vitro model reported earlier (Trofimova et al., 2010), the current study aimed to evaluate whether acute inhibition of α-KGDHC by intra-CA_1 injection of SP could attenuate cognitive decline induced by Aβ in rats. We also determined the activity of α-KGDHC, GDH, and GS that is robustly associated with neurotransmission, energy metabolism, and learning and memory deficit in AD pathology.

2. Material and methods

2.1. Animals

Adult male Wistar rats (230–250 g) were obtained from the animal house colony of the Pasteur Institute of Iran (Tehran, Iran). To prevent performance bias, they were housed randomly, and four rats were kept in each cage with free access to food and water. The rats were maintained on a reverse 12 h light/dark cycle, in a controlled temperature (23 ± 2 °C) and humidity. Baseline characteristics of all animals were the same, and randomly assigned to each group ($n = 6$–8/group). The sample size was calculated from power analysis of the data as previously obtained in our lab. Experiments were performed according to the Guideline for the Care and Use of Laboratory Animals (National Research Council, 2011). The protocols for this experimental research were confirmed by the ethics committee of the Shahid Beheshti University of Medical Sciences (IR.SBMU.MSP.REC.1397. 570).

2.2. Surgery

Male Wistar rats were anesthetized by injection of ketamine (100 mg/kg) and xylazine (10 mg/kg, IP). Cannulation was performed using stereotaxic surgery in the CA_1 region of the dorsal hippocampus according to the Paxinos and Watson Atlas (AP: −3.84, L: ±2.2, and DV: −2.7) (Paxinos, 2005). Stainless steel cannulas (23 gauge) were bilaterally implanted 1 mm above the CA1 region. Cannulas were fixed to the skull using screws and dental cement. An internal obturator was used after cannulation to prevent the cannula from being blocked.

2.3. Drug administration and experimental procedures

Human Amyloid $beta_{25–35}$ peptide (Sigma, USA) was dissolved in sterile 0.9 % saline at a concentration of 5 μg/2 μl and then aliquoted and stored in −20 °C. The aliquots were incubated at 37 °C for four days to produce Aβ aggregation (Hooshmandi et al., 2018). The intra-hippocampal injections were performed for four successive days using a 5 μl Hamilton syringe connected to a 30-gauge needle which was inserted 1 mm above the tip of the cannula and to facilitate the drug release, the needle remained in place for one more minute before retracted gently. For the intra-hippocampal injection, rats were given 2 μl of Aβ (5 μg/1 μl) or saline as the control group on each side, for 4 consecutive days started from the first day of surgery. Different doses of succinyl phosphatase (SP, Medchem, USA) was dissolved in distilled water as a stock solution, and administered intra-hippocampally 30 min after the first $Aβ_{25–35}$ microinjection, or 1 h after each training session.

For evaluation of time-dependent effects of SP, two sets of experiments were carried out i.e.: post-treatment and co-treatment protocols. In the post-treatment protocol, seven days post-injection of $Aβ_{25–35}$, rats received an intra-CA_1 injection of different doses of SP including four logarithmic doses of SP (10 nM, 100 nM, 100 μM, and 1000 μM) or vehicle in three consecutive days 1 h after each training session. For the co-treatment protocol, SP (10 nM) was administrated just 30 min after the first $Aβ_{25–35}$ injection. For the assessment of any weight change during the study, the animal's weight was monitored in 4 stages: 1) before surgery 2) 4 days after surgery 3)10 days after surgery 4) before sacrifice. A schematic diagram of the experimental procedure is presented in Scheme 1.

2.4. Morris water maze

2.4.1. Apparatus

The Morris water maze (MWM) consisted of a pool (150 cm diameter, 70 cm height) with dark and smooth inner surfaces full of water (19 ± 3 °C) until 25 cm lower than the arena's edge. The hidden Plexiglas platform (10 cm diameter) was submerged approximately 2 cm under the water's surface in a fixed position in the middle of the goal quadrant. The maze was placed in an indirect lighting room with fixed distal cues including a cupboard, curtain, several pictures on the wall, etc., as a navigation point reference for finding the target, independent of the start point. For recording the experiments, a CCD camera (Panasonic Inc., Japan) located above the center point of the arena, was used, and locomotion tracking was measured by the Ethovision software (version XT 7.1, Noldus, the Netherlands).

2.4.2. Behavioral procedure

For habituation, rats were allowed to swim for 60 s in the pool without the platform one day before the training (Gholamipour-Badie

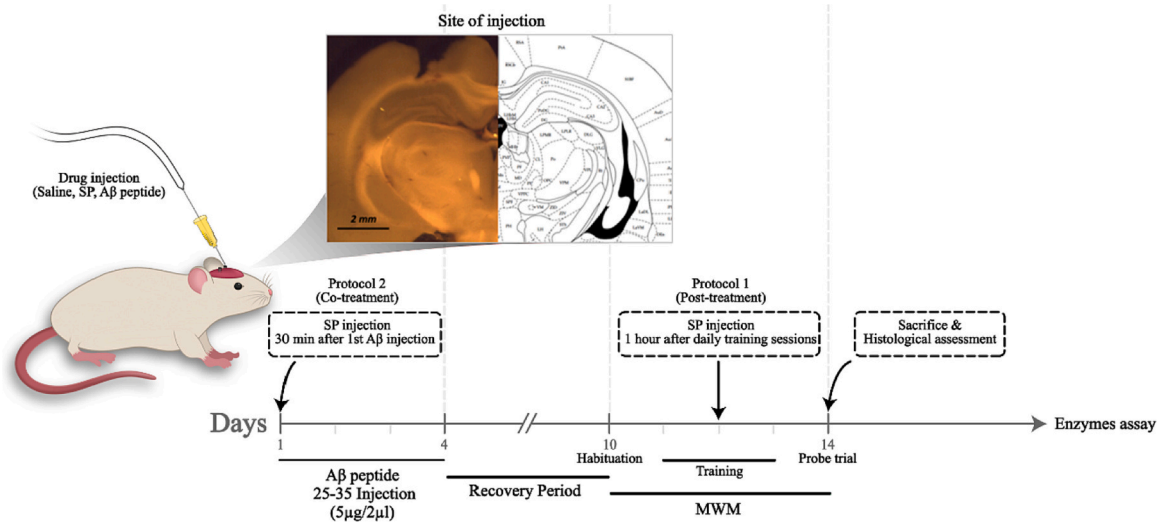

Scheme 1. Time line for Experimental procedures.
Protocol 1 is the procedure for post-treatment injections and protocol 2 is related to co-treatment injections.

et al., 2013; Nategh et al., 2015). In the acquisition phase, the platform was placed in the target zone throughout the three consecutive days, and animals were released into the pool (nose to maze wall) randomly from different zones (the software divided the arena into four zones). One training block consisted of 4 trials with 10 min inter-trial intervals. Rats were allowed to swim in the tank and find the platform for 60 s. If animals did not find the platform during the 60 s, they were guided to it and were allowed to stand there for 20 s before removing them from the pool. For the retention session, 24 h after the last day of training, the platform was removed, and animals were released in the pool in the opposite quadrant from the platform location. Time in the target quadrant, escape latency, area under the curve, and velocity were recorded for data analysis. For the visuomotor activity assessment, after the probe test, the platform was raised over the water surface, coated by shiny aluminum foil, and the animals were allowed to swim for 60 s and find the visible platform. All experiments were done between 9:00 and 13:00 h.

2.5. Tissue preparation

At the end of the behavioral assessment, rats from each group were anesthetized by CO_2 inhalation, then decapitated. Hippocampi were extracted, rinsed with phosphate buffer saline (PBS), and stored in liquid nitrogen for 24 h and then at −80 °C until the enzyme assessment.

Three rats from each group were used for histopathological studies. For this purpose, rats were subjected to deep anesthesia followed by cardiac perfusion with 10 mM ice-cold PBS (pH = 7.4) and 4 % paraformaldehyde (PFA). The brain samples were then fixed in PFA at 4 °C. After 72 h, gradient dehydration and embedding of tissue in paraffin was performed at 59 °C. Tissue was coronally sectioned with the thickness of 5–7 μm.

2.6. Enzyme assay

Both right and left hippocampal tissues were homogenized three times (each one 60 s) using an ice-cold lysis buffer including a complete protease inhibitor cocktail; the lysates were then homogenated and centrifuged separately in conditions specific to each enzyme, and stored overnight in −80 °C. For the detection of protein concentration, the method of Bradford was used (Bradford, 1976). The number of biologically independent replicates for each group was three, and each sample was replicated three times.

2.6.1. α-KGDHC enzyme activity assay

α-KGDHC enzyme activity was measured according to Gibson et al. study (Gibson et al., 1988) with some modification. In this method, alpha-glutarate is converted to succinyl-coenzyme in presence of α-KGDHC, and NAD is converted to NADH. Tris buffer solution (50 mM, pH:7), MgCl2 (1 mM), CaCl2 (1 mM), K-EDTA (0.5 mM), dithiothreitol (1 mM), triton X-100 (1 %), thiamine pyrophosphate (0.3 mM), co-enzymes (0.163 mM), and 2-ketoglutarate (1.25 mM) was the components of reaction solution. The reaction was started by adding NAD as substrate, and NADH formation was monitored at 340 nm for 20 min by 30 s intervals, and the enzyme activity was expressed in μmol/min/mg protein (Gibson et al., 1988).

2.6.2. GDH enzyme activity assay

GDH activity was measured according to Arce et al. (1988). In this method, glutamate is converted to alpha-ketoglutarate in the presence of the GDH enzyme, which monitors the rate of NADH formation at 340 nm. The reaction mixture consisted of a diluted sample supernatant, potassium phosphate buffer solution (0.1 M, pH:7), alpha-ketoglutarate (0.1 M), NH_4Cl (1 mM) where reaction started with adding NADH (10 mg/L), and the enzyme activity was reported in terms of μmol/min/mg protein (Arce et al., 1990).

2.6.3. GS enzyme activity assay

GS enzyme activity was measured according to Pamiljans et al. (1962) methods (Pamiljans et al., 1962). The GS activity was determined based on the γ-glutamyl hydroxamate production (Petito et al., 1992). The reaction mixture included 200 μl of diluted sample supernatant with glutamate (700 mM), ATP (40 mM), and hydroxylamine (40 mM) in assay buffer (40 mM imidazole pH 7.4, 20 mM $MgCl_2$, 1 mM DTT, and 0.01 % Triton X-100) was prepared with a negative control without glutamate. After incubation at 37 °C for 30 min, reactions were stopped by the addition of $FeCl_3$, trichloroacetic acid, and HCl. After delaying for color development, density was measured at a wavelength of 540 nm. Enzyme activity was reported in terms of μmol/h/mg protein.

2.7. Histochemical staining

In order to assess the neuropathological effects of drugs used in this study histochemical staining of different parts of the hippocampus was performed. The tissue sections were deparaffinized and then hydrated with xylene followed by incubation with 0.1 % cresyl Violet solution (Nissl Staining, Sigma-Aldrich, USA) at 58 °C for 6 min (Miller et al.,

2013; Sanati et al., 2019). Dehydration of tissue sections was then carried out with the help of increasing concentration of ethanol followed by washing with xylene and then covered with cover-slip. Using Nikon light microscope, 5–7 stained tissue sections from each animal were selected from 2.7 to 3.7 mm posterior to the bregma. The regions of interest including CA1, CA3, and DG were evaluated. The images were processed through ImageJ software to quantify the number of surviving and dead neurons. At least 3 brain sections from each animal ($n = 3$ rats per group) was used to count the number of surviving neurons in the CA1, CA3, and DG regions of hippocampus at 200× magnification.

2.8. Statistical analysis

Data were analyzed by Graph Pad Software (Ver. 8.0) and presented as the mean ± SEM (Standard Error of Mean). Two-way analysis of variance (ANOVA) with repeated measures followed by post hoc analysis (Tukey's test) was applied for the data of the MWM training days. Also, one-way (ANOVA) followed by Tukey multi-comparison test was used to compare differences between the groups in the MWM probe session and molecular assessments. For swimming pattern Matlab software (Ver. 2015.a) was used. $P < 0.05$ was considered to be statistically significant as demonstrated on the graphs by symbols. One symbol (* or # or ^) represents $P < 0.05$, two symbols (** or ## or ^^) represent $P < 0.01$ and three symbols (*** or ### or ^^^) represent $P < 0.001$.

3. Results

3.1. Effects of different doses of SP on spatial learning and memory in rats

To see the effects of Succinyl Phosphonate (SP) on spatial learning and memory processes using the MWM task, four logarithmic doses of SP (10 nM, 100 nM, 100 μM, 1000 μM) were chosen and injected into the CA_1 area for three consecutive days. Two-way repeated-measures ANOVA revealed no significant effect of treatment at the acquisition trials (Data not shown). However, in the probe test, there was a significant difference in treatment effect between groups [$F_{(4,\ 25)} = 4.669$, $P = 0.005$], using a one-way ANOVA test. Tukey's post hoc analysis showed that dose (100 μM, $P < 0.01$) disrupted the spatial memory and decreased the time spent in the target zone, while 10 nM, 100 nM, and 1000 μM had no significant effect on spatial memory. It should be noted that no difference was found between sham-operated and intact groups in the behavioral tests. Therefore, sham-operated group that received saline (as solvent of amyloid-beta and SP) was considered as the control group for the rest of study. In addition, we observed that there was no significant difference in body weight among each group during the experiments from day 0 to 14.

3.2. Post-treatment of SP did not have any significant effect on Aβ-induced memory deficit

After observing the adverse effects of the $A\beta_{25-35}$ on spatial learning

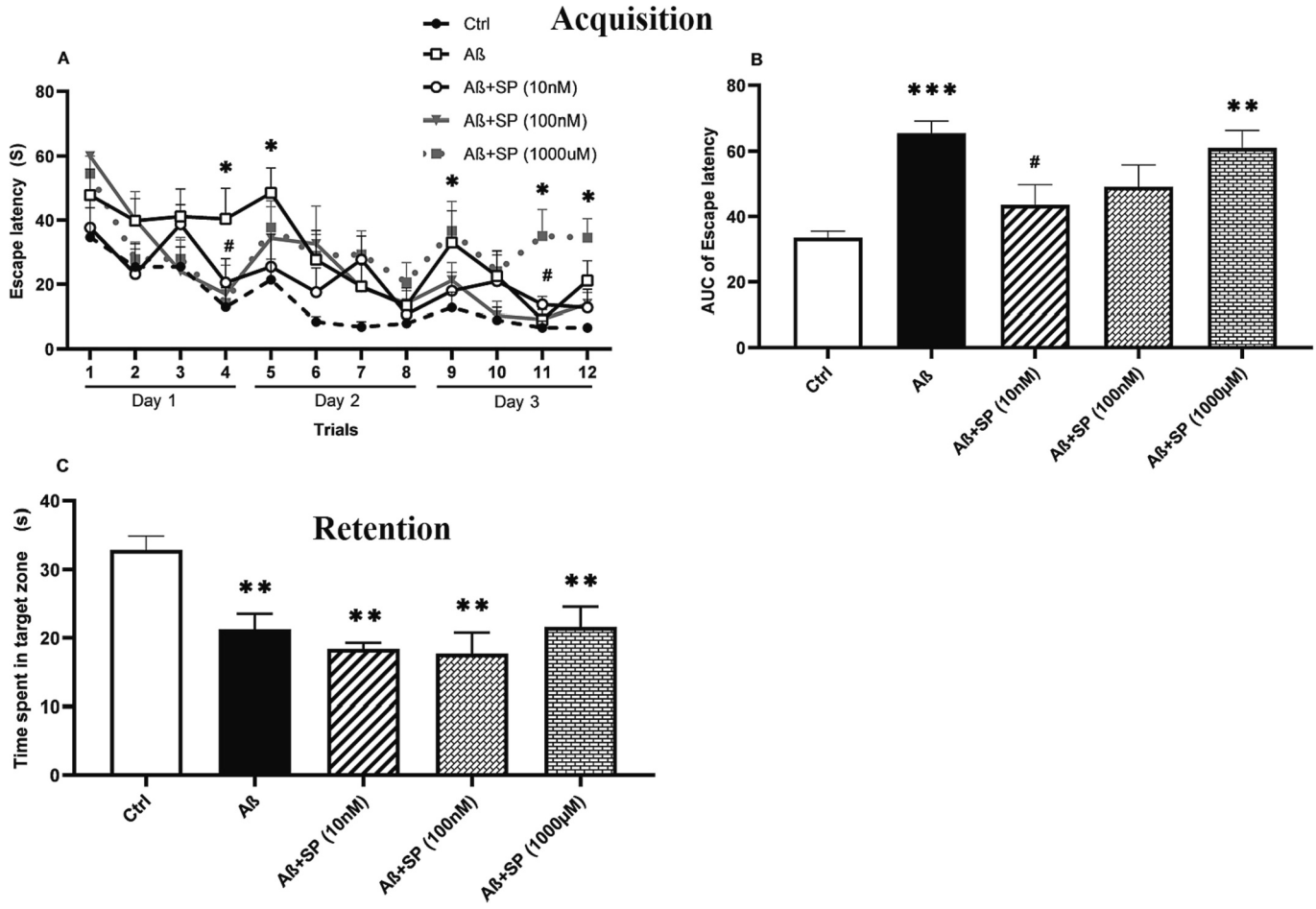

Fig. 1. The effect of post-Aβ injection of SP on spatial learning and memory using Morris water maze task.
A) Escape latency to find the submerged platform over 12 trials for three consecutive days. B) Area-under-the-curve (AUC) for the escape latencies for 12 trials over 3 days during the acquisition phase (four trials per day). C) Time spent in target zone in the probe phase. Data are presented in the form of mean ± SEM ($n = 6$–8 per group). *$P < 0.05$, **$P < 0.01$, ***$P < 0.001$, vs. control; #P < 0.05, ##P < 0.01, ###P < 0.001 vs $A\beta_{25-35}$.

and memory, we used post-treatment strategies. Seven days after the last injection of $A\beta_{25-35}$, SP (10 nM, 100 nM, and 1000 μM) was injected into the CA_1 area 1 h after the last trial each day. Two-way ANOVA showed that the effects of treatment and time were significant ($P < 0.001$). However, the effect of treatment × time interaction was not significant [$F_{(44,370)} = 0.981$, $P = 0.508$] Fig. 1A. Further analysis with Tukey's post test revealed that SP at doses of 10 nM, and 100 nM, but not 1000 μM, improved acquisition of the task in rats treated with $A\beta_{25-35}$. Tukey's post hoc analysis showed that there were significant differences in the 4th, 5th, and 9th trials for the $A\beta_{25-35}$, and in the 11th and 12th trials for the $A\beta_{25-35}$ + SP (1000 μM) group compared to the control group ($P < 0.05$). For further analysis of learning curves, the areas under the

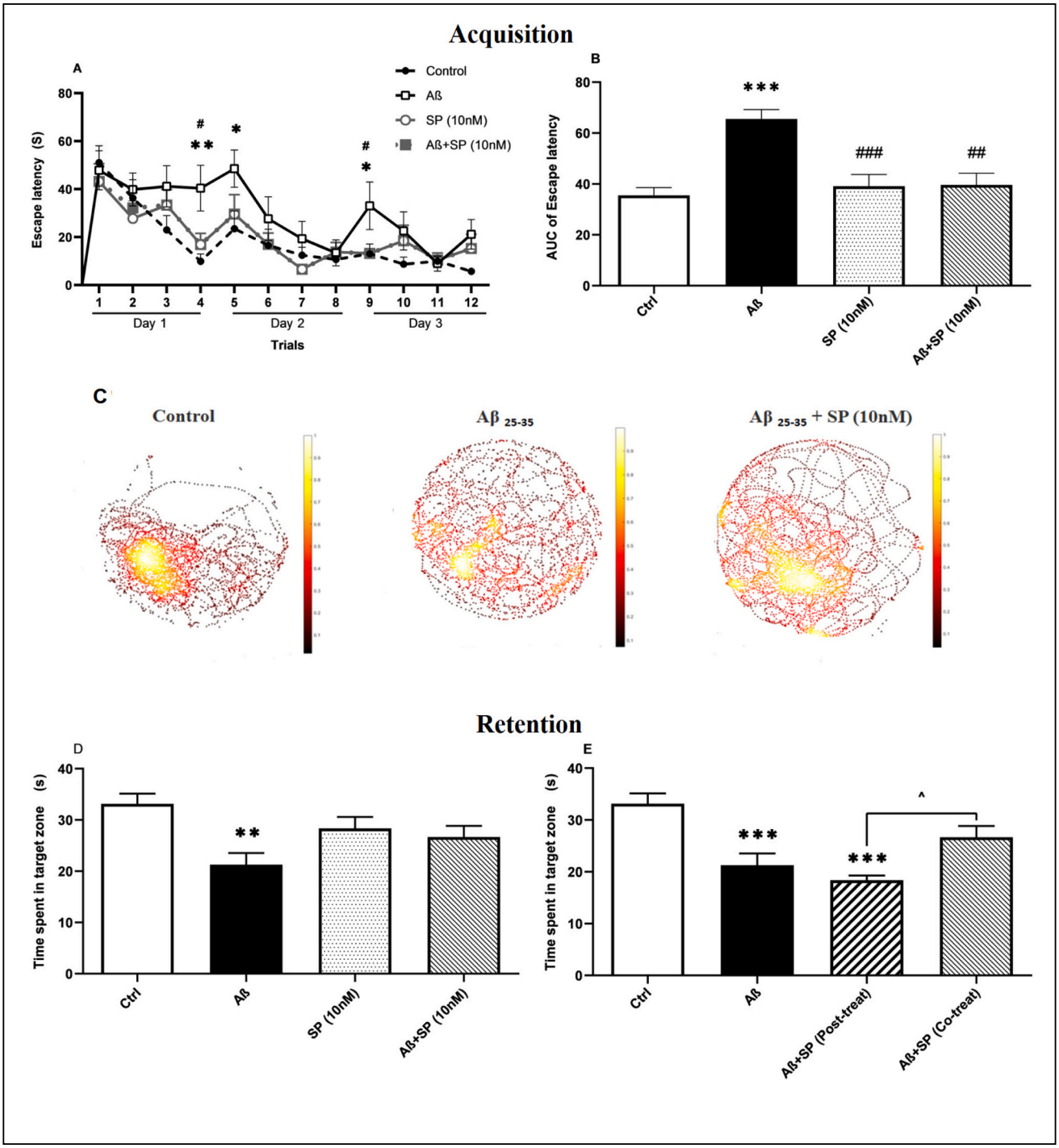

Fig. 2. The effect of intra-hippocampal co-injection of SP (10 nM) and $A\beta_{25-35}$ on spatial learning and memory in the Morris water maze task.
A) Escape latency to find the submerged platform over 12 trials for three consecutive days. B) Area-under-the-curve (AUC) for the escape latencies for 12 trials over 3 days during the acquisition phase (four trials per day). C) Representative images of movement traces of rats in the experimental groups. The redder color displays the longer the rats spent in each quadrant, and the cooler colors shows a shorter duration. The yellow circle shows the position where the platform was located previously. D, E) Time spent in target zone in the retention test. Data are presented in the form of mean ± SEM ($n = 6$–8 per group). $^*P < 0.05$, $^{**}P < 0.01$, $^{***}P < 0.001$, vs. control; #P < 0.05, ##P < 0.01, ###P < 0.001, vs. $A\beta_{25-35}$; $\hat{}P < 0.05$ co-treat vs. post-treat. (For interpretation of the references to color in this figure legend, the reader is referred to the web version of this article.)

curves (AUCs) were also analyzed for 12 trials during the learning phase using one-way ANOVA [$F_{(4, 29)} = 7.541$, $P < 0.001$] Fig. 1B. The AUC of the escape latency curves was significantly elevated in the $A\beta_{25–35}$ ($P < 0.00$), and $A\beta_{25–35}$ + SP (1000 μM) ($p < 0.01$) groups in comparison with the control group ($P < 0.05$). However, the AUC of SP at a dose of 10 nM was significantly lowered with respect to the $A\beta_{25–35}$ group ($P < 0.05$) and tended towards the control group. Finally, Tukey's multiple comparisons post-test between $A\beta_{25–35}$ and post-treatment group showed there was a significant difference between the $A\beta_{25–35}$ + SP (10 nM) group compared to the $A\beta_{25–35}$ group in the AUC curve ($P < 0.05$). However, no difference of task acquisition was found between the $A\beta_{25–35}$ and $A\beta_{25–35}$ + SP except in the 4th and 11th trials ($P < 0.05$) for the high dose SP (1000 μM) treatment.

In the retention test, there was a significant difference between all doses with the control group [$F_{(4, 30)} = 6.981$, $P = 0.0004$] Fig. 1C, and time spent in the target quadrant was decreased in all doses compared to the control group, indicating that SP in post-treatment condition could not reverse the retention deficit due to $A\beta_{25–35}$ treatment.

3.3. Co-treatment of SP (10 nM) with Aβ could reverse Aβ-induced learning and memory deficit

In the next step, the preventive effect of SP was evaluated. SP (10 nM) was injected 30 min after the first $A\beta_{25–35}$ injection, to see whether SP could prevent $A\beta_{25–35}$ learning and memory deficit. We chose this dose because of the better performance of animals in the previous protocol. As shown in Fig. 2, SP (10 nM) per se had no significant effect on spatial learning and memory, probably due to the ceiling effect in which the control group performed at the highest level and SP could not further increase the performance. However, the results of two-way ANOVA within the groups showed that there is a significant difference in the treatment factor [$F_{(3, 324)} = 9.052$, $P < 0.0001$]. There are significant differences in the 4th and 9th trials in SP (10 nM) and $A\beta_{25–35}$ + SP (10 nM) treated animals compared to the $A\beta_{25–35}$ treated group ($P < 0.05$) Fig. 2A. For further analysis, the areas under the curves (AUCs) were also analyzed for 12 trials during the learning phase using one-way ANOVA [$F_{(4, 33)} = 11.88$, $P < 0.001$] Fig. 2B. The AUC was significantly greater in the $A\beta_{25–35}$ group in comparison with the control group ($P < 0.001$). However, no significant difference in the AUC of escape latency curves was found between the control and SP groups, indicating SP could reverse the $A\beta_{25–35}$ induced learning deficit ($P < 0.001$). Tukey's multiple comparisons post-test between $A\beta_{25–35}$ and co-treatment group showed there was a significant difference between $A\beta_{25–35}$ + SP (10 nM) compared to the $A\beta_{25–35}$ group in the AUC curve ($P < 0.001$).

Twenty-four hours after the last training trial, the platform was removed, and a probe test for measuring spatial reference memory was conducted. Fig. 2C demonstrates heat maps of movement traces for experimental groups. Unlike Aβ treated group, control rats focused on the target quadrant and seemed closer to the platform location. Treatment of the Aβ group with SP could bring the swimming search profile closer to the control group.

One-way ANOVA has shown a significant difference between groups [$F_{(3, 26)} = 5.141$, $P = 0.0063$]. Tukey's multiple comparisons post-test showed there was a significant difference for the Aβ group compared to the control group in time spent in the target zone, and the rats spent less time in the target zone in comparison to the control group ($p < 0.05$) Fig. 2D. However, the escape latency in the SP and $A\beta_{25–35}$ + SP groups was not different from the control, indicating that SP treatment could reverse the $A\beta_{25–35}$ deficit. No significant difference was found between the $A\beta_{25–35}$ and in the SP or $A\beta_{25–35}$ + SP groups.

Finally, one way ANOVA revealed a significant difference of target quadrant duration between the post- and, co-treatment groups in the retention test [$F_{(3,312)} = 7.893$, $P < 0.001$]. Time spent in target quadrant was decreased in the $A\beta_{25–35}$ + SP post-treatment compared to the co-treatment group, indicating that unlike SP post-treatment, concomitant administration of SP with $A\beta_{25–35}$ prevents Aβ induced memory deficit (Fig. 2E).

3.4. $A\beta_{25–35}$ or SP administration did not alter velocity and visuomotor performance of animals

To recognize the possible effects of drug injection on the visuospatial performance, their swimming speed was calculated. No significant difference was seen in swimming speed among experimental groups in the probe test, indicating intact motor abilities of the treated animals [$F_{(3.26)} = 1.491$, $P = 0.240$] Fig. 3A.

Finally, to check out the sensory-motor activities, coordination, and animals motivation, a visible platform test was done after the probe test. The data showed that all animals could find the platform with almost the same latency, indicating their normal visual/motor activity. [$F_{(3, 21)} = 0.176$, $P = 0.911$] Fig. 3B.

3.5. SP co-treatment but not post-treatment could increase α-KGDHC activity that reduced in the $A\beta_{25–35}$ treated group

After performing the behavioral assessment, rats were sacrificed, and enzyme activity in the extracted hippocampus was measured. To prevent detection bias, animals were selected randomly for enzyme activity assessment. There were significant differences in α-KGDHC activity [$F_{(4, 24)} = 17.97$, $P < 0.0001$] between groups. Post hoc analysis by Tukey multiple comparison test showed that α-KGDHC activity was decreased in $A\beta_{25–35}$, and $A\beta_{25–35}$ + SP (post-treatment) groups compared to the control group ($p < 0.001$), and there were significant increases in α-KGDHC activity between the SP (10 nM) ($P < 0.001$), and $A\beta_{25–35}$ + SP (co-treatment) ($P < 0.01$) groups compared to the $A\beta_{25–35}$ treated group. But there was no significant difference between SP (10 nM) and $A\beta_{25–35}$ + SP (co-treatment) vs control. As shown in Fig. 4, the enzyme activity of the $A\beta_{25–35}$ + SP (co-treatment) group was similar to the control group, while the activity of the $A\beta_{25–35}$ + SP (Post-treatment) group was similar to the $A\beta_{25–35}$ group, indicating the advantage of co-treatment over post-treatment strategy.

3.6. SP co-treatment prevented the increase of GDH activity induced by $A\beta_{25–35}$ toxicity

There was a significant difference between the experimental groups using one-way ANOVA [$F_{(4, 36)} = 5.413$, $P < 0.001$]. As shown in Fig. 5, Tukey multiple comparison post-test revealed that GDH activity increased in the $A\beta_{25–35}$ ($P < 0.01$) and $A\beta_{25–35}$ + SP (post-treatment) groups compared to the control group ($P < 0.01$). But the enzyme activity decreased in the $A\beta_{25–35}$ + SP (co-treatment) group compared to the $A\beta_{25–35}$ group ($P < 0.05$), while SP (10 nM), and $A\beta_{25–35}$ + SP (co-treatment) groups were not different from control.

3.7. GS activity decreased significantly by $A\beta_{25–35}$ toxicity; SP co-treatment could prevent this reduction

The enzyme activity of GS, a cytosolic enzyme, showed significant differences between groups [$F_{(4, 14)} = 7.331$, $p = 0.002$] using one-way ANOVA. Post hoc analysis showed that $A\beta_{25–35}$ administration alone and in combination with SP in the post-treatment group resulted in a significant decrease in GS activity compared to the control group ($P < 0.01$). SP co-treatment significantly reversed this reduction ($P < 0.05$). Also, there were no significant differences between $A\beta_{25–35}$ + SP (post-treatment) groups compared to the $A\beta_{25–35}$ group, and $A\beta_{25–35}$ + SP (co-treatment) compared to the control group, Fig. 6.

3.8. Observation of Nissl staining

The tissue sections were prepared from brain samples collected on the 14th day after microinjection of the reagents to assess the extent of

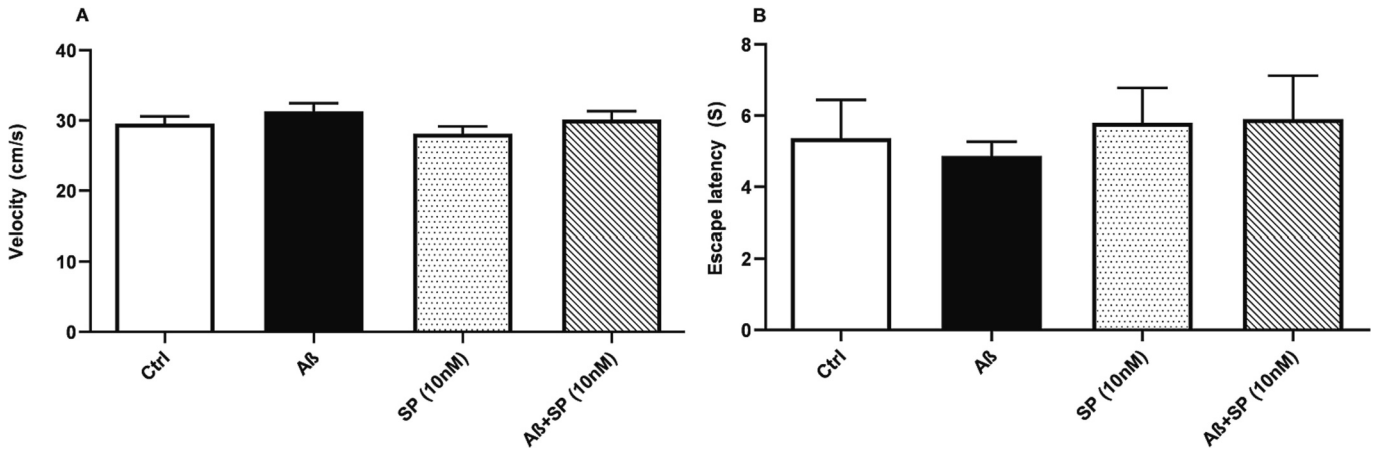

Fig. 3. The effect of SP (10 nM) administration on velocity and visuomotor performance.
A) Swimming speed in the probe test of the MWM task, and B) Escape Latency of animals for assessing visuomotor activity of animals in visible platform test. Data are presented as mean ± SEM (n = 6–8).

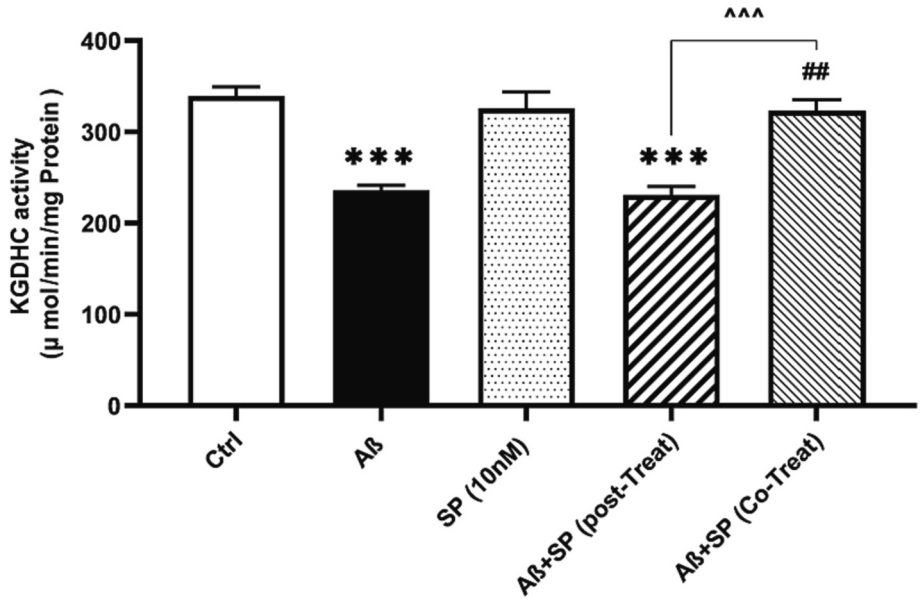

Fig. 4. The effect of SP treatment on the hippocampal α-ketoglutarate dehydrogenase complex (α-KGDHC) activity.
Data are presented as mean ± SEM. ($n = 3$ rat per group, 9 experiment). $^{*}P < 0.05$, $^{**}P < 0.01$, $^{***}P < 0.001$, vs. control; $\#P < 0.05$, $\#\#P < 0.01$, $\#\#\#P < 0.001$, vs. $A\beta_{25-35}$. $\hat{}\hat{}\hat{}P < 0.001$. Between groups.

neuronal damage in the hippocampal formation in different experimental groups. Fig. 7A shows representative images of Nissl stained hippocampal formation in different groups. Surviving neurons were characterized by well-defined round shaped cells having nucleolus and typical Nissl bodies in the cytoplasm whereas dead neurons were recognized by massive shrinkage, dense cytoplasm, dark nucleus, and abnormal morphology. Analysis of data by one-way ANOVA revealed that the Aβ-treated rats exhibited a significantly reduced percentage of surviving neurons as compared to the control rats ($P < 0.001$) Fig. 7B. The Aβ group showed an increased number of dark Nissl-stained neurons with massive shrinkage and aberrant morphology in the CA1 and DG regions of the hippocampus. Furthermore, the post-treated rats also exhibited an increased number of dark neurons as compared to the control rats ($P < 0.001$). However, SP ($P < 0.001$) and SP co-treated ($P < 0.01$) groups showed noticeable improved hippocampal morphology compared to the Aβ group as evident by uniformly stained and tidily arranged hippocampal neuronal cells. Also, the number of surviving neurons of the SP co-treatment group in the DG region of the hippocampus was increased compared with the Aβ group ($P < 0.01$) Fig. 7C and D.

4. Discussion

Here, we examined whether regulation of α-KGDHC activity by SP administration in the CA_1 area could be beneficial for modulating the major pathological events in a rat model of AD. The experimental model used in our study was induced by microinjection of Aβ into the hippocampus, an important cerebral structure that is involved in the early phase of AD mainly due to the overproduction and accumulation of Aβ. This approach is a common method that has been accepted and used in many literatures as an AD-like model in rodents (Hooshmandi et al., 2018; Gholamipour-Badie et al., 2013; Khonacha et al., 2022). One of the main advantages of this model is that it targets directly the specific brain regions e.g. hippocampus, and other brain areas remain intact, so it makes feasible to investigate amyloidopathy in different brain regions. In our study, we aimed to examine α-KGDHC action in amyloidopathy

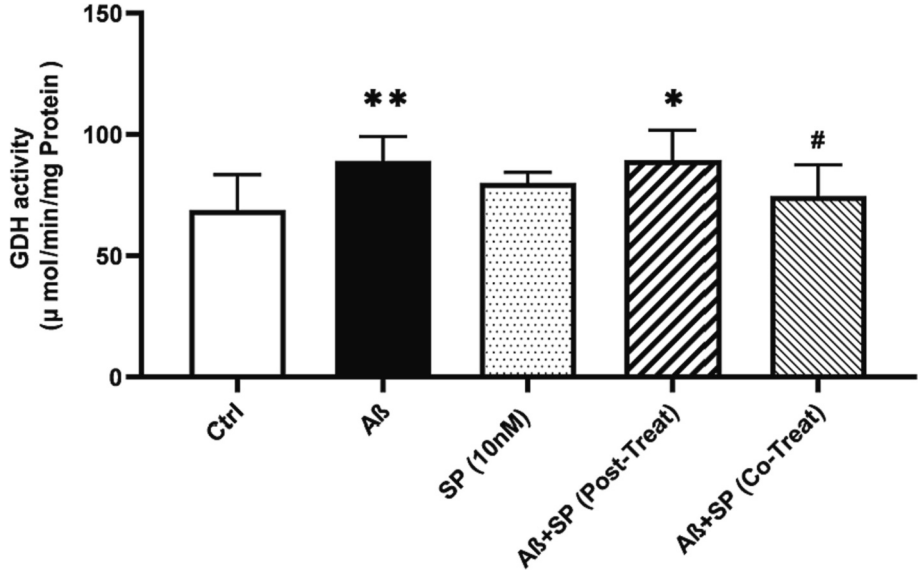

Fig. 5. The effect of SP treatment on the hippocampal Glutamate Dehydrogenase (GDH) activity.
Data are presented as mean ± SEM. (n = 3 per group). *$P < 0.05$, **$P < 0.01$, ***$P < 0.001$, vs. control; #P < 0.05, ##P < 0.01, ###P < 0.001, vs. $A\beta_{25-35}$.

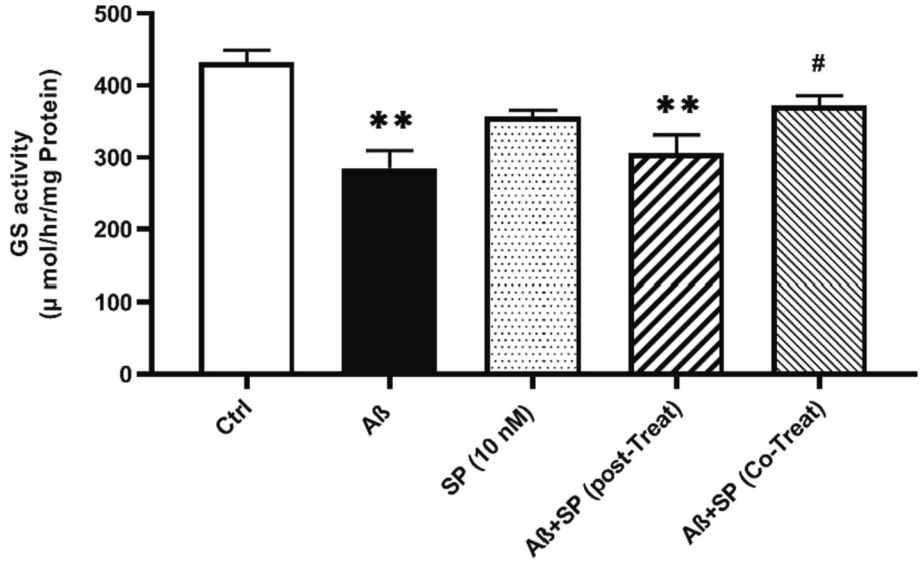

Fig. 6. The effect of SP treatment on the hippocampal Glutamine synthetase (GS) activity.
Data are represented as mean ± SEM. *P < 0.05, **P < 0.01, ***P < 0.001, vs. control; #P < 0.05, ##P < 0.01, ###P < 0.001, vs. $A\beta_{25-35}$.

state induced locally in the hippocampus which is an accepted sporadic AD model.

Mitochondria as a primary source of energy production in the cells are responsible for several cellular functions that could be a potential therapeutic target in the early stages of AD (Cadonic et al., 2016). Decreased activity of α-KGDHC about 30–75 % has been reported in damaged and undamaged cerebral regions in AD patients which might be associated with decreased brain metabolism (Gibson et al., 1988). However, inhibition of α-KGDHC appears to be protective if cells are along with facing life-threatening conditions (Gibson et al., 2010). SP as a phosphonate analog of α-ketoglutarate is shown to specifically inhibit α-KGDHC (Bunik et al., 2005; Bunik et al., 1992), and is used for modeling the conditions for manipulation of enzyme activity (Gibson et al., 2012; Santos et al., 2006).

Our behavioral results showed that Aβ injection in the dorsal CA_1 area decelerated the MWM task acquisition and disrupted spatial memory. Post-treatment by SP improved learning of $A\beta_{25-35}$ treated rats in two doses (10 nM, 100 nM), but SP in 1000 μM deteriorated learning. However, it did not reverse the Aβ impairing effect on spatial memory performance at any of above-mentioned doses. It seems, that daily injection of SP may cause a cumulative effect and its or its metabolite level reached a toxic level to disrupt memory. In confirmation, we observed that SP at the higher doses deteriorated learning and memory performances. To further examine the possible protective effect of a minimum effective dose of SP on Aβ pathology, 10 nM SP was chosen. Interestingly, administration of SP 30 min post-Aβ injection improved learning in the Aβ treated group. Besides, it reversed spatial memory deficit induced by Aβ suggesting a preventive effect of SP at lower doses on Aβ pathology in the brain.

In a study by Trofimova et al., behavioral changes in open field, closed and elevated plus maze tests were examined 4 and 24 h after treatment with different doses of SP in healthy male rats. Their results generally indicated an elevation in exploratory activity, decreased anxiety, and better orientation in rats subjected to 5 mg/kg of SP while

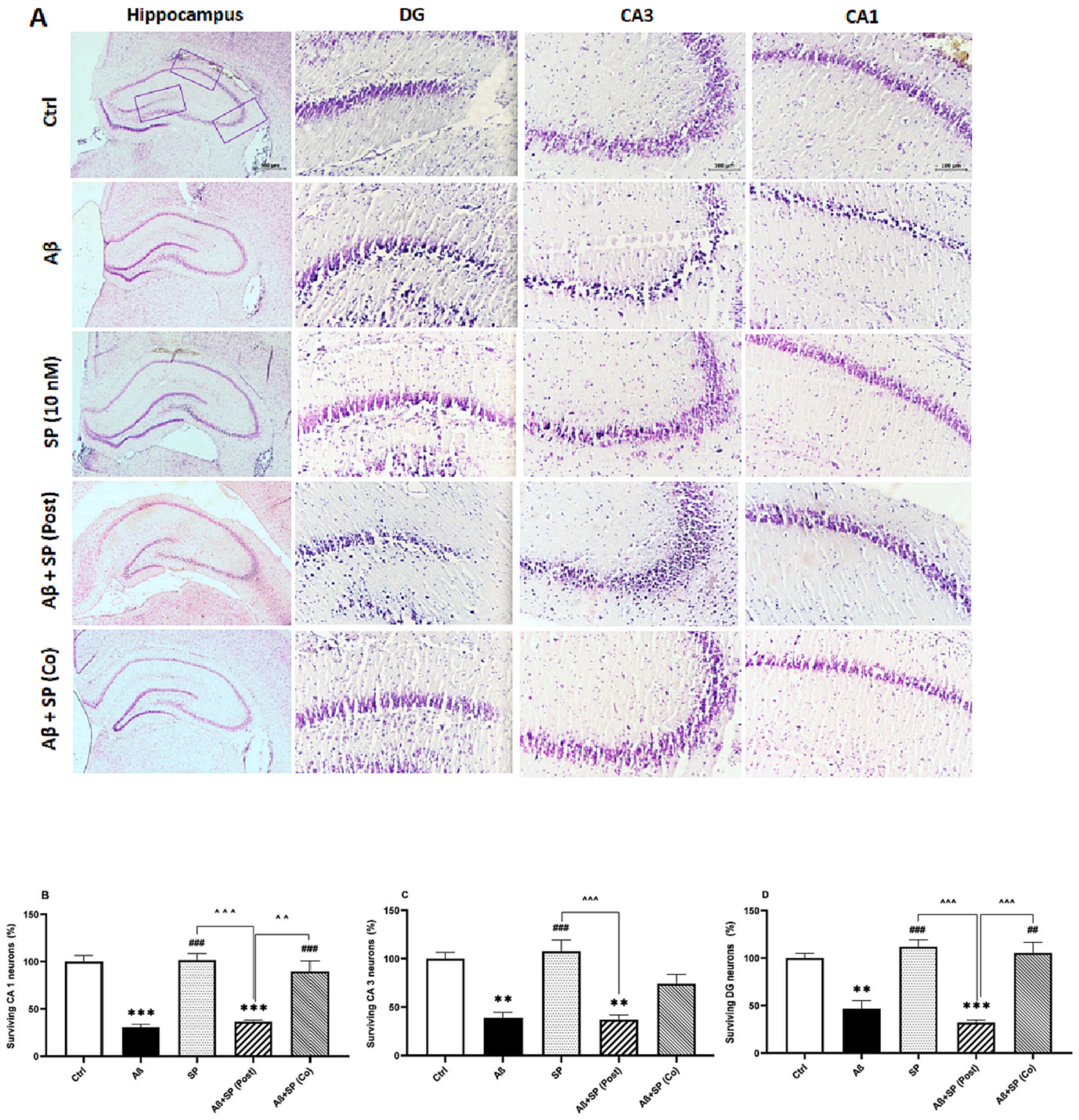

Fig. 7. Hippocampal morphological changes following Aβ toxicity and the effect of SP on the histopathology of different areas of the hippocampus. A) Nissl staining was applied to identify Nissl bodies and the extent of neuronal damage in the hippocampus (×4), CA3, DG, and CA1 regions (×20) subfields. Scale bar = 500 μm (general), 100 μm (regions). DG, dentate gyrus; Ctrl, control; Aβ, amyloid β; SP, Succinyl Phosphonate. B) The surviving cell numbers in the CA1 region. C) The surviving cell numbers in the CA3 region. D) The surviving cell numbers in the DG region. Data are represented as mean ± SEM. *P < 0.05, **P < 0.01, ***P < 0.001, vs. control; #P < 0.05, ##P < 0.01, ###P < 0.001, vs. $A\beta_{25-35;}$ ^P < 0.05, ^^P < 0.01, ^^^P < 0.001 vs. SP post-treat.

the increasing dose to 25 mg/kg developed a deteriorative effect on the above-mentioned tasks (Trofimova et al., 2010). They proposed that SP at low doses may up-regulate α-KGDHC in a compensatory response and ultimately improve the behavioral function. Furthermore, in this study SP pre-treatment in pregnant rats 45–50 min before exposure to hypoxia, have led to abrogation of nearly all impaired behavioral parameters induced by hypoxia in the open field test (Trofimova et al., 2010).

Since the activity of this enzyme in the brain is sex-dependent, its inhibition may produce different results in the females (Trofimova et al., 2010). It should be considered that there may be differences in the organization and function of hippocampal neural circuits in both sexes. Based on a study by Hawley et al. (2012), an important difference in spatial learning and memory between male and female Wistar rats appears to be that they use different learning approaches that are controlled by different areas of the brain. The preference of adult male rats is a hippocampal-dependent spatial strategy rather than a striatum-

dependent response strategy. In contrast, female rats prefer a spatial strategy only when the concentration of estradiol in their bloodstream increases (Hawley et al., 2012; Safari et al., 2021). The difference in the structure and function of the hippocampus in males and females may be partly due to the difference in their distribution and activity of α-KGDHC, which needs to be elucidated in future studies.

Our data shows that the Aβ induced learning and spatial memory deficit is accompanied by a decrease in α-KGDHC activity. In agreement to our study, it has been reported that treatment of rats with streptozotocin (STZ) or corticosterone resulted in impairment of references and working memories in the hole boar test, and the α-KGDHC activity was decreased in both treatments (Hoyer and Lannert, 2008). Also, non-spatial memory impairment in the animal model of amyloid pathology was associated with a decrease in TCA cycle enzymes activity including α-KGDHC along with defects in mitochondrial biogenesis markers (Shaerzadeh et al., 2014). In contrast to our results, Dumont et al. (2009) have shown that dihydrolipoyl succinyltransferase deficiency that leads to a reduction of α-KGDHC activity, could not impair spatial learning and memory in the MWM task in male mice in a transgenic mouse model of AD (Dumont et al., 2009).

It has been reported that the α-KGDHC activity is reduced in human with neurodegenerative disorders (Bubber et al., 2005; Gibson et al., 1988; Gibson et al., 2013; Gibson et al., 2000). As mentioned above, the activity of α-KGDHC was reduced in the Aβ group. According to our results, SP in combination with Aβ in the co-treatment group compensated this reduction, and increased α-KGDHC activity towards the control level. It seems that compensatory responses to α-KGDHC inhibition is due to the additive effect of cellular responses against metabolic stress that leads to activation of internal mechanisms, such as increasing its synthesis or leading to posttranslational alterations like the amino acid side chain changes (Trofimova et al., 2010). This occurrence could be interpreted by the fact that SP, can protect α-KGDHC from an irreversible inactivation that occurs during its catalysis (Kabysheva et al., 2009). Our obtained results confirmed this suggested mechanism as well.

Conversely, it seems that a decrease in α-KGDHC in the post-treatment group may result in exhausting cellular compensatory mechanisms in various pathological conditions, and the metabolism is disrupted and cells become more sensitive to metabolic stress (Graf et al., 2013; Banerjee et al., 2016). It's a matter of time, as we observed. So, the metabolism is disrupted and cells become more sensitive to metabolic stresses. Collectively, it seems that the effect of SP on neurons is dose and time-dependent, and is affected by various types of stress and the stage of diseases. Perhaps it could illustrate the non-identical and occasionally contrasting results obtained with different experimental protocols. Nevertheless, more studies should be done to find the reason for the change in the activity of α-KGDHC in SP treated rats at different time intervals in both male and female animals.

To further elucidate the mechanism of action of SP, the activity of some key enzymes involved in neurotransmission and energy metabolism in the AD, upon pre- and post-treatment with SP were assessed. GDH as a crucial enzyme for glutamate homeostasis in the brain, which is a converter of a Krebs cycle intermediate α-KG to glutamate, is playing a critical role in providing energy for cells. A decline or increase in GDH activity can modulate the energy metabolism of cells and affects the early onset of neurodegenerative diseases such as AD (Kim and Baik, 2019; McLain et al., 2011; Miulli et al., 1993). Our GDH assay showed that Aβ could increase GDH activity. A single dose of SP alone has no effect, but in combination with Aβ in the co-treatment group, the enzyme activity decreased towards the control level.

Graf et al., have shown that SP treatment in pregnant rats as a pre-treatment model, abrogated most of the physiologic and morphologic hypoxia-induced changes such as glutamate excitotoxicity in the offspring brains (Graf et al., 2009). Also, overexpression of GDH1 can lead to morphological alterations in neurons such as the decline of the axon terminal and dendritic spine in the CA_1 region (Bao et al., 2009; Plaitakis et al., 2013). This is in line with our behavioral results that declined activity of α-KGDHC in Aβ or the post-treatment group, caused an increase in GDH activity. In our study SP alone did not affect GDH activity, this is similar to Bunik et al. (2005), results that the reaction rate with SP for bovine GDH has not been changed (Bunik et al., 2005). Conversely, a study by Lander et al. (2020) have shown the GDH deficiency by homozygous deletion of Glud1 in mice impairs recognition memory, because of c-Fos reduction in the pyramidal neurons of the CA_1 area (Lander et al., 2020). Given this evidence, SP may affect the GDH activity under metabolic stress, and the cells can employ several levels of GDH regulation to the flux of glutamate.

In our study, in the Aβ and post-treatment groups, the activity of GS was decreased, and this reduction was prevented in the co-treatment group and reached to the control level. The reduction of GS activity which is the rate-limiting enzyme that converts glutamate to glutamine leads to an elevation in GABA and glutamate in the brain which may lead to glutamate neurotoxicity (Jayakumar and Norenberg, 2016). It is demonstrated that changes in GS activity and its gene expression, are accompanied by excitotoxicity, which is observed in several neurologic diseases, including AD (Le Prince et al., 1995; Robinson, 2000; Jacob et al., 2007; Lievens et al., 2001). As we detected the GDH level profoundly increased in Aβ injected group. It is possible that in this condition, the activity of GS, the rate-limiting enzyme that converts glutamate to glutamine is diminished (Schousboe et al., 2014). Further, in the histological assessment we found that Aβ induced profound cell loss in the hippocampus. The results are in line with reports indicating that the amyloid beta-mediated cell loss occurred in the hippocampi which may lead to behavioral deficits (Reifert et al., 2011; Calvo-Flores Guzmán et al., 2020). Our data shows co-treatment of Aβ with SP, but not post-treatment, protected neuronal cells against Aβ toxicity. This finding indicates that SP protected the neuronal cells against Aβ when it used concomitantly and before the occurrence of severe neurotoxicity, but after the establishment of neurotoxicity, it is no longer able to reverse the Aβ effect.

In a study, GS inhibition in a time close to synaptogenesis led to memory impairment in the novel place recognition (NOR) test (Son et al., 2019). Disruption in the NOR test may be associated with lower GS expression in the dorsal hippocampus of aged mice (Soontornniyomkij et al., 2016). Ivens et al. (2019) study, reported that GS inhibition may imitate the adolescent stress effects on CA1-LTP in brain slices from intact rats (Ivens et al., 2019). In addition, treatments of Wistar rats with lanthanum chloride ($LaCl_3$) led to decrease in GS and spatial learning and memory impairment (Hu et al., 2018). Besides, Gibbs's study suggested that the impairment in memory consolidation in the Aβ group may be due to a decrease in GS activity (Gibbs et al., 1996). This hypothesis could be an explanation for our data as well. In the Aβ and post-treatment groups, the activity of GS was decreased, and this reduction was prevented in the co-treatment group. However, the SP administration did not change the activity of GS in the SP group. GS dependency on ATP could be a reason for the reduced activity of GS as a result of α-KGDHC decreased activity, which suppresses the Krebs cycle and decreases ATP production (Jayakumar and Norenberg, 2016). Similar to our study, some reports indicate that declined GS activity in the brains of AD patients drives GS oxidation by Aβ and is related to neuritic plaques in the cortex of AD patients' brains (Robinson, 2000; Castegna et al., 2002). Therefore, it seems that decreased activity of GS in the late and advanced stages of AD can be a sign of alteration in glutamatergic neurotransmission, which gives rise to an imbalance in hippocampal neurotransmitters that leads to impairments in memory in AD patients (Olabarria et al., 2011), which is similar to what we obtained in the behavioral section. Contrary to the mentioned studies, inhibition of GS did not impair recognition memory, although temporal dependent memory was changed (Kant et al., 2014), and chronic inhibition of GS was not related to learning and memory deficit in mice (Blin et al., 2002). The direct effect of AD and other neurologic diseases on GS expression in astrocytes leads to a compensatory reaction that causes de novo expression of GS in neurons (Robinson, 2000; Robinson, 2001).

From findings of the current study, and according to the reports from other investigators, it can be suggested that inhibition of α-KGDHC by SP leads to intra-mitochondrial accumulation of 2-oxoglutarate as a compensatory response, and may be a self-regulatory mechanism against the decrease in α-KGDHC activity (Kumar et al., 2003), which accelerate its more efficient use in the TCA cycle. Further, α-ketoglutarate is transaminated to leucine, valine, and GABA, and may have a role in supply of carbon for the GS. Mild reduction of α-KGDHC may accelerate glycolysis, and bypasses the TCA cycle through the GABA shunt, and/or conversion of valine to succinate (Chen et al., 2016; Bunik and Strumilo, 2009; Mailloux et al., 2016). Furthermore, moderate inhibition of α-KGDHC using SP, dampens calcium deregulation induced by glutamate in a concentration- and time-dependent manner, and could act as a buffer, and leads to the attenuation of metabolic mismatch caused by the changes in α-KGDHC activity (Kabysheva et al., 2009).

In summary, the present study shows that under the condition of Aβ pathology in the hippocampal CA_1 area, SP in specific doses, and time-dependently preserved learning and memory performance at the early stage of Aβ toxicity and decelerates the disease progression possibly through the regulation of glutamate-glutamine homeostasis. This aspect needs to be further addressed in detail in future studies.

5. Limitations and future directions

Indeed, one of the limitations of our work is that we performed the experiment in male rats only, in the futures studies gender difference should be considered, while investigating the role of α-KGDHC activity in AD. Moreover, SP is the structural analog of α-KGDHC which affects the activity of this enzyme in the complex form (Trofimova et al., 2012). Since, α-KGDHC is the combination of three sub-enzymes, then it is desirable to identify the role of each subunit in the onset and progression of AD.

CRediT authorship contribution statement

Fatemeh Sayehmiri: Investigation, data collection, analysis, writing the original draft. Fereshteh Motamedi, and Fariba Khodagholi: Conceptualization, Methodology, interpretation of data, Supervision, and Fund acquisition. Nima Naderi, and Hamid Gholamipour-Badie: Conceptualization, Methodology, interpretation of data. Reza Hashemi: Morris Water Maze experiments. Faezeh Aliakbarzadeh, and Soudabeh Naderi: molecular section. All authors revised and approved the final version of the manuscript.

Declaration of competing interest

None.

Data availability

The authors do not have permission to share data.

Acknowledgment

The authors are thankful to the Neuroscience Research Center at the Shahid Beheshti University of Medical Science for supporting this work as part of the Ph.D. dissertation of Fatemeh Sayehmiri.

Funding

This study was funded by Research Affairs of Shahid Beheshti University of Medical Sciences, Tehran, Iran.

References

Albers, D.S., Augood, S.J., Park, L.C., Browne, S.E., Martin, D.M., Adamson, J., et al., 2000. Frontal lobe dysfunction in progressive supranuclear palsy: evidence for oxidative stress and mitochondrial impairment. J. Neurochem. 74 (2), 878–881.

Arce, C., Canadas, S., Oset-Gasque, M., Castro, E., Gonzalez, M., 1990. Glutamate dehydrogenase: some properties of the rat brain enzyme from different cellular compartments. Comp. Biochem. Physiol. C Comp. Pharmacol. Toxicol. 97 (2), 265–267.

Banerjee, K., Munshi, S., Xu, H., Frank, D.E., Chen, H.-L., Chu, C.T., et al., 2016. Mild mitochondrial metabolic deficits by α-ketoglutarate dehydrogenase inhibition cause prominent changes in intracellular autophagic signaling: potential role in the pathobiology of Alzheimer's disease. Neurochem. Int. 96, 32–45.

Bao, X., Pal, R., Hascup, K.N., Wang, Y., Wang, W.T., Xu, W., et al., 2009. Transgenic expression of Glud1 (glutamate dehydrogenase 1) in neurons: in vivo model of enhanced glutamate release, altered synaptic plasticity, and selective neuronal vulnerability. J. Neurosci. 29 (44), 13929–13944.

Blin, M., Crusio, W.E., Hévor, T., Cloix, J.F., 2002. Chronic inhibition of glutamine synthetase is not associated with impairment of learning and memory in mice. Brain Res. Bull. 57 (1), 11–15.

Bradford, M.M., 1976. A rapid and sensitive method for the quantitation of microgram quantities of protein utilizing the principle of protein-dye binding. Anal. Biochem. 72 (1–2), 248–254.

Bubber, P., Haroutunian, V., Fisch, G., Blass, J.P., Gibson, G.E., 2005. Mitochondrial abnormalities in Alzheimer brain: mechanistic implications. Ann. Neurol. 57 (5), 695–703.

Bunik, V., Biryukov, A., Zhukov, Y.N., 1992. Inhibition of pigeon breast muscle α-ketoglutarate dehydrogenase by phosphonate analogues of α-ketoglutarate. FEBS Lett. 303 (2–3), 197–201.

Bunik, V.I., Strumilo, S., 2009. Regulation of catalysis within cellular network: metabolic and signaling implications of the 2-oxoglutarate oxidative decarboxylation. Curr. Chem. Biol. 3 (3), 279–290.

Bunik, V.I., Denton, T.T., Xu, H., Thompson, C.M., Cooper, A.J., Gibson, G.E., 2005. Phosphonate analogues of α-ketoglutarate inhibit the activity of the α-ketoglutarate dehydrogenase complex isolated from brain and in cultured cells. Biochemistry 44 (31), 10552–10561.

Cadonic, C., Sabbir, M.G., Albensi, B.C., 2016. Mechanisms of mitochondrial dysfunction in Alzheimer's disease. Mol. Neurobiol. 53 (9), 6078–6090.

Calvo-Flores Guzmán, B., Elizabeth Chaffey, T., Hansika Palpagama, T., Waters, S., Boix, J., Tate, W.P., et al., 2020. The interplay between beta-amyloid 1–42 (Aβ (1–42))-induced hippocampal inflammatory response, p-tau, vascular pathology, and their synergistic contributions to neuronal death and behavioral deficits. Front. Mol. Neurosci. 13, 522073.

Castegna, A., Aksenov, M., Aksenova, M., Thongboonkerd, V., Klein, J.B., Pierce, W.M., et al., 2002. Proteomic identification of oxidatively modified proteins in Alzheimer's disease brain. Part I: creatine kinase BB, glutamine synthase, and ubiquitin carboxy-terminal hydrolase L-1. Free Radic. Biol. Med. 33 (4), 562–571.

Chen, H., Denton, T.T., Xu, H., Calingasan, N., Beal, M.F., Gibson, G.E., 2016. Reductions in the mitochondrial enzyme α-ketoglutarate dehydrogenase complex in neurodegenerative disease–beneficial or detrimental? J. Neurochem. 139 (5), 823–838.

Dumont, M., Ho, D.J., Calingasan, N.Y., Xu, H., Gibson, G., Beal, M.F., 2009. Mitochondrial dihydrolipoyl succinyltransferase deficiency accelerates amyloid pathology and memory deficit in a transgenic mouse model of amyloid deposition. Free Radic. Biol. Med. 47 (7), 1019–1027.

Gholamipour-Badie, H., Naderi, N., Khodagholi, F., Shaerzadeh, F., Motamedi, F., 2013. L-type calcium channel blockade alleviates molecular and reversal spatial learning and memory alterations induced by entorhinal amyloid pathology in rats. Behav. Brain Res. 237, 190–199.

Gibbs, M.E., O'Dowd, B.S., Hertz, L., Robinson, S.R., Sedman, G.L., Ng, K.T., 1996. Inhibition of glutamine synthetase activity prevents memory consolidation. Brain Res. Cogn. Brain Res. 4 (1), 57–64.

Gibson, G., Kingsbury, A., Xu, H., Lindsay, J., Daniel, S., Foster, O., et al., 2003. Deficits in a tricarboxylic acid cycle enzyme in brains from patients with Parkinson's disease. Neurochem. Int. 43 (2), 129–135.

Gibson, G.E., Sheu, K.-F.R., Blass, J.P., Baker, A., Carlson, K.C., Harding, B., et al., 1988. Reduced activities of thiamine-dependent enzymes in the brains and peripheral tissues of patients with Alzheimer's disease. Arch. Neurol. 45 (8), 836–840.

Gibson, G.E., Zhang, H., Sheu, K.F., Bogdanovich, N., Lindsay, J.G., Lannfelt, L., et al., 1998. Alpha-ketoglutarate dehydrogenase in Alzheimer brains bearing the APP670/671 mutation. Ann. Neurol. 44 (4), 676–681.

Gibson, G.E., Park, L.C., Sheu, K.-F.R., Blass, J.P., Calingasan, N.Y., 2000. The α-ketoglutarate dehydrogenase complex in neurodegeneration. Neurochem. Int. 36 (2), 97–112.

Gibson, G.E., Starkov, A., Blass, J.P., Ratan, R.R., Beal, M.F., 2010. Cause and consequence: mitochondrial dysfunction initiates and propagates neuronal dysfunction, neuronal death and behavioral abnormalities in age-associated neurodegenerative diseases. Biochim. Biophys. Acta 1802 (1), 122–134.

Gibson, G.E., Chen, H.-L., Xu, H., Qiu, L., Xu, Z., Denton, T.T., et al., 2012. Deficits in the mitochondrial enzyme α-ketoglutarate dehydrogenase lead to Alzheimer's disease-like calcium dysregulation. Neurobiol. Aging 33 (6), 1121. e13–e24.

Gibson, G.E., Hirsch, J.A., Cirio, R.T., Jordan, B.D., Fonzetti, P., Elder, J., 2013. Abnormal thiamine-dependent processes in Alzheimer's disease. Lessons from diabetes. Mol. Cell. Neurosci. 55, 17–25.

Graf, A., Kabysheva, M., Klimuk, E., Trofimova, L., Dunaeva, T., Zündorf, G., et al., 2009. Role of 2-oxoglutarate dehydrogenase in brain pathologies involving glutamate neurotoxicity. J. Mol. Catal. B Enzym. 61 (1), 80–87.
Graf, A., Trofimova, L., Loshinskaja, A., Mkrtchyan, G., Strokina, A., Lovat, M., et al., 2013. Up-regulation of 2-oxoglutarate dehydrogenase as a stress response. Int. J. Biochem. Cell Biol. 45 (1), 175–189.
Hawley, W.R., Grissom, E.M., Barratt, H.E., Conrad, T.S., Dohanich, G.P., 2012. The effects of biological sex and gonadal hormones on learning strategy in adult rats. Physiol. Behav. 105 (4), 1014–1020.
Hooshmandi, E., Motamedi, F., Moosavi, M., Katinger, H., Zakeri, Z., Zaringhalam, J., et al., 2018. CEPO-fc (an EPO derivative) protects hippocampus against Aβ-induced memory deterioration: a behavioral and molecular study in a rat model of Aβ toxicity. Neuroscience 388, 405–417.
Hoyer, S., Lannert, H., 2008. Long-term effects of corticosterone on behavior, oxidative and energy metabolism of parietotemporal cerebral cortex and hippocampus of rats: comparison to intracerebroventricular streptozotocin. J. Neural Transm. 115 (9), 1241.
Hu, X., Yang, J., Sun, Y., Gao, X., Zhang, L., Li, Y., et al., 2018. Lanthanum chloride impairs memory in rats by disturbing the glutamate-glutamine cycle and over-activating NMDA receptors. Food Chem. Toxicol. 113, 1–13.
Ivens, S., Çalışkan, G., Papageorgiou, I., Cesetti, T., Malich, A., Kann, O., et al., 2019. Persistent increase in ventral hippocampal long-term potentiation by juvenile stress: a role for astrocytic glutamine synthetase. Glia 67 (12), 2279–2293.
Jacob, C., Koutsilieri, E., Bartl, J., Neuen-Jacob, E., Arzberger, T., Zander, N., et al., 2007. Alterations in expression of glutamatergic transporters and receptors in sporadic Alzheimer's disease. J. Alzheimers Dis. 11 (1), 97–116.
Jayakumar, A.R., Norenberg, M.D., 2016. Glutamine synthetase: role in neurological disorders. The glutamate/GABA-glutamine. Cycle 327–350.
Kabysheva, M.S., Storozhevykh, T.P., Pinelis, V.G., Bunik, V.I., 2009. Synthetic regulators of the 2-oxoglutarate oxidative decarboxylation alleviate the glutamate excitotoxicity in cerebellar granule neurons. Biochem. Pharmacol. 77 (9), 1531–1540.
Kant, D., Ss, Tripathi, Qureshi, M.F., Tripathi 2nd, S., Pandey, S., Singh, G., et al., 2014. The effect of glial glutamine synthetase inhibition on recognition and temporal memories in the rat. Neurosci. Lett. 560, 98–102.
Khonacha, S.E., Mirbehbahani, S.H., Rahdar, M., Davoudi, S., Borjkhani, M., Khodagholi, F., et al., 2022. Kisspeptin-13 prevented the electrophysiological alterations induced by amyloid-beta pathology in rat: possible involvement of stromal interaction molecules and pCREB. Brain Res. Bull. 184, 13–23.
Kim, A.Y., Baik, E.J., 2019. Glutamate dehydrogenase as a neuroprotective target against neurodegeneration. Neurochem. Res. 44 (1), 147–153.
Kumar, M.J., Nicholls, D.G., Andersen, J.K., 2003. Oxidative α-ketoglutarate dehydrogenase inhibition via subtle elevations in monoamine oxidase B levels results in loss of spare respiratory capacity: implications for Parkinson's disease. J. Biol. Chem. 278 (47), 46432–46439.
Lander, S.S., Chornyy, S., Safory, H., Gross, A., Wolosker, H., Gaisler-Salomon, I., 2020. Glutamate dehydrogenase deficiency disrupts glutamate homeostasis in hippocampus and prefrontal cortex and impairs recognition memory. Genes Brain Behav. 19 (6), e12636.
Le Prince, G., Delaere, P., Fages, C., Lefrançois, T., Touret, M., Salanon, M., et al., 1995. Glutamine synthetase (GS) expression is reduced in senile dementia of the Alzheimer type. Neurochem. Res. 20 (7), 859–862.
Lievens, J.-C., Woodman, B., Mahal, A., Spasic-Boscovic, O., Samuel, D., Kerkerian-Le Goff, L., et al., 2001. Impaired glutamate uptake in the R6 Huntington's disease transgenic mice. Neurobiol. Dis. 8 (5), 807–821.
Mailloux, R.J., Ayre, D.C., Christian, S.L., 2016. Induction of mitochondrial reactive oxygen species production by GSH mediated S-glutathionylation of 2-oxoglutarate dehydrogenase. Redox Biol. 8, 285–297.
Mastrogiacomo, F., Bergeron, C., Kish, S.J., 1993. Brain alpha-ketoglutarate dehydrogenase complex activity in Alzheimer's disease. J. Neurochem. 61 (6), 2007–2014.
McLain, A.L., Szweda, P.A., Szweda, L.I., 2011. α-Ketoglutarate dehydrogenase: a mitochondrial redox sensor. Free Radic. Res. 45 (1), 29–36.
Miller, J.A., Nathanson, J., Franjic, D., Shim, S., Dalley, R.A., Shapouri, S., et al., 2013. Conserved molecular signatures of neurogenesis in the hippocampal subgranular zone of rodents and primates. Development 140 (22), 4633–4644.
Miulli, D.E., Norwell, D.Y., Schwartz, F.N., 1993. Plasma concentrations of glutamate and its metabolites in patients with Alzheimer's disease. J. Am. Osteopath. Assoc. 93 (6), 670–676.
Nategh, M., Nikseresht, S., Khodagholi, F., Motamedi, F., 2015. Nucleus incertus inactivation impairs spatial learning and memory in rats. Physiol. Behav. 139, 112–120.
National Research Council, 2011. Committee for the Update of the Guide for the C, Use of Laboratory A. The National Academies Collection: Reports funded by National Institutes of Health. Guide for the Care and Use of Laboratory Animals. Washington (DC): National Academies Press (US) Copyright © 2011. National Academy of Sciences.
Nilsen, L.H., Shi, Q., Gibson, G.E., Sonnewald, U., 2011. Brain [U-13C] glucose metabolism in mice with decreased α-ketoglutarate dehydrogenase complex activity. J. Neurosci. Res. 89 (12), 1997–2007.
Olabarria, M., Noristani, H.N., Verkhratsky, A., Rodríguez, J.J., 2011. Age-dependent decrease in glutamine synthetase expression in the hippocampal astroglia of the triple transgenic Alzheimer's disease mouse model: mechanism for deficient glutamatergic transmission? Mol. Neurodegener. 6 (1), 1–9.
Pamiljans, V., Krishnaswamy, P., Dumville, G., Meister, A., 1962. Studies on the mechanism of glutamine synthesis; isolation and properties of the enzyme from sheep brain. Biochemistry 1 (1), 153–158.
Park, L.C., Albers, D.S., Xu, H., Lindsay, J.G., Beal, M.F., Gibson, G.E., 2001. Mitochondrial impairment in the cerebellum of the patients with progressive supranuclear palsy. J. Neurosci. Res. 66 (5), 1028–1034.
Paxinos, G.W.C., 2005. The Rat Brain in Stereotaxic Coordinates. Elsevier/Academic press.
Petito, C.K., Chung, M.C., Verkhovsky, L.M., Cooper, A.J.L., 1992. Brain glutamine synthetase increases following cerebral ischemia in the rat. Brain Res. 569 (2), 275–280.
Plaitakis, A., Zaganas, I., Spanaki, C., 2013. Deregulation of glutamate dehydrogenase in human neurologic disorders. J. Neurosci. Res. 91 (8), 1007–1017.
Reifert, J., Hartung-Cranston, D., Feinstein, S.C., 2011. Amyloid beta-mediated cell death of cultured hippocampal neurons reveals extensive Tau fragmentation without increased full-length tau phosphorylation. J. Biol. Chem. 286 (23), 20797–20811.
Robinson, S.R., 2000. Neuronal expression of glutamine synthetase in Alzheimer's disease indicates a profound impairment of metabolic interactions with astrocytes. Neurochem. Int. 36 (4–5), 471–482.
Robinson, S.R., 2001. Changes in the cellular distribution of glutamine synthetase in Alzheimer's disease. J. Neurosci. Res. 66 (5), 972–980.
Safari, S., Ahmadi, N., Mohammadkhani, R., Ghahremani, R., Khajvand-Abedeni, M., Shahidi, S., et al., 2021. Sex differences in spatial learning and memory and hippocampal long-term potentiation at perforant pathway-dentate gyrus (PP-DG) synapses in Wistar rats. Behav. Brain Funct. 17 (1), 9.
Sanati, M., Khodagholi, F., Aminyavari, S., Ghasemi, F., Gholami, M., Kebriaeezadeh, A., et al., 2019. Impact of gold nanoparticles on amyloid β-induced Alzheimer's disease in a rat animal model: involvement of STIM proteins. ACS Chem. Neurosci. 10 (5), 2299–2309.
Santos, S.S., Gibson, G.E., Cooper, A.J., Denton, T.T., Thompson, C.M., Bunik, V.I., et al., 2006. Inhibitors of the α-ketoglutarate dehydrogenase complex alter [1-13C] glucose and [U-13C] glutamate metabolism in cerebellar granule neurons. J. Neurosci. Res. 83 (3), 450–458.
Schousboe, A., Scafidi, S., Bak, L.K., Waagepetersen, H.S., McKenna, M.C., 2014. Glutamate metabolism in the brain focusing on astrocytes. Adv Neurobiol. 11, 13–30.
Shaerzadeh, F., Motamedi, F., Khodagholi, F., 2014. Inhibition of akt phosphorylation diminishes mitochondrial biogenesis regulators, tricarboxylic acid cycle activity and exacerbates recognition memory deficit in rat model of Alzheimer's disease. Cell. Mol. Neurobiol. 34 (8), 1223–1233.
Shi, Q., Risa, Ø., Sonnewald, U., Gibson, G.E., 2009. Mild reduction in the activity of the α-ketoglutarate dehydrogenase complex elevates GABA shunt and glycolysis. J. Neurochem. 109, 214–221.
Son, H., Kim, S., Jung, D.-H., Baek, J.H., Lee, D.H., Roh, G.S., et al., 2019. Insufficient glutamine synthetase activity during synaptogenesis causes spatial memory impairment in adult mice. Sci. Rep. 9 (1), 252.
Soontornniyomkij, V., Kesby, J.P., Soontornniyomkij, B., Kim, J.J., Kisseleva, T., Achim, C.L., et al., 2016. Age and high-fat diet effects on glutamine synthetase immunoreactivity in liver and hippocampus and recognition memory in mice. Curr. Aging Sci. 9 (4), 301–309.
Trofimova, L., Lovat, M., Groznaya, A., Efimova, E., Dunaeva, T., Maslova, M., et al., 2010. Behavioral impact of the regulation of the brain 2-oxoglutarate dehydrogenase complex by synthetic phosphonate analog of 2-oxoglutarate: implications into the role of the complex in neurodegenerative diseases. Int. J. Alzheimers Dis. 2010.
Trofimova, L.K., Araújo, W.L., Strokina, A.A., Fernie, A.R., Bettendorff, L., Bunik, V.I., 2012. Consequences of the α-ketoglutarate dehydrogenase inhibition for neuronal metabolism and survival: implications for neurodegenerative diseases. Curr. Med. Chem. 19 (34), 5895–5906.
Xiao, D., Zeng, L., Yao, K., Kong, X., Wu, G., Yin, Y., 2016. The glutamine-alpha-ketoglutarate (AKG) metabolism and its nutritional implications. Amino Acids 48 (9), 2067–2080.